Fundamental Studies on the Runoff by Characteristics

AUTHOR(S):

IWAGAKI, Yuichi

CITATION:

IWAGAKI, Yuichi. Fundamental Studies on the Runoff by Characteristics. Bulletins - Disaster Prevention Research Institute, Kyoto University 1955, 10: 1-25

ISSUE DATE:

1955-12-10

URL:

http://hdl.handle.net/2433/123659

DISASTER PREVENTION RESEARCH INSTITUTE
BULLETIN No. 10 DECEMBER, 1955

FUNDAMENTAL STUDIES ON THE RUNOFF ANALYSIS BY CHARACTERISTICS

BY

YUICHI IWAGAKI

KYOTO UNIVERSITY, KYOTO, JAPAN

Errata

Bulletin No. 10

Page 6, Eq. (7)′,

for $u=\sqrt{\left(\frac{5}{3}-\frac{4}{3}\frac{R}{B}\right)\frac{qR^{4/3}}{2n^2gh}}+\cdots\cdots$ read $u=\sqrt{\left\{\left(\frac{5}{3}-\frac{4}{3}\frac{R}{B}\right)\frac{qR^{4/3}}{2n^2gh}\right\}^2+\cdots\cdots}$

〃 10, line 9 from the foot, for $\frac{du}{dt}$ read $\frac{\partial u}{\partial t}$

〃 18, line 2, 〃 distrubance 〃 disturbance

〃 19, 〃 〃, 〃 Lahoratory 〃 Laboratory

〃 23, Ep. (31),

for $u=\sqrt{\left\{\left(1+\frac{2}{3\beta}\right)\frac{q^*R^{4/3}}{2n^2gA}\right\}+\cdots\cdots}$ read $=\sqrt{\left\{\left(1+\frac{2}{3\beta}\right)\frac{q^*R^{4/3}}{2n^2gA}\right\}^2+\cdots\cdots}$

DISASTER PREVENTION RESEARCH INSTITUTE
KYOTO UNIVERSITY
BULLETINS

Bulletin No. 10 December, 1955

Fundamental Studies on the Runoff Analysis by Characteristics

By
Yuichi IWAGAKI

Contents

Synopsis

In treating the hydraulic analysis of surface runoff phenomena, the author's basic idea is expressed as follows: the surface runoff mechanism of rain water in a mountainous district consists of the combination of overland flow and flow in open channels with lateral inflow. Consequently, the unsteady flows with lateral inflow must be solved for various conditions, individually.

In this paper, an approximate method for calculation of unsteady flow in open channels with lateral inflow, using the characteristic curve, is presented. Hydrographs resulting from the abrupt increase and decrease of rate of lateral inflow are obtained by this approach, and moreover the calculated hydrographs are compared with the experimental results.

1. Introduction

It is one of the most important and difficult problems in the field of hydrology and practical river engineering to establish the essential features of rainfall-runoff relations. Up to the present day, many researches on such problems have been performed and various empirical formulas and methods available for the practical purpose have been proposed.

There are, among recent researches on this subject, two different approaches for analysis of rainfall-runoff relation: one is for the overland flow introduced by Izzard[1], Izzard and Augustine[2], Horner and Jens[3] and Hicks[4], and the other is based upon the unit hydrograph method first presented by Sherman in 1932. Especially the latter is considered a highly effective and simple tool for hydrologic work in the United States of America, and is being actively utilized even in Japan. However, the hydraulic rationality of this method has not yet been approved and the question is whether it may be naturally applied to steep rivers in Japan or not. On the other hand, the analytical approach for overland flow developed by Izzard is used only when the flow is laminar at all times[6], but the theoretical basis of this analysis is not so sound.

Rain water on the ground surface pours into seas or lakes through small and large tributaries and other streams. Hence, the mechanism of surface runoff in a mountainous district falls generally into two parts: (1) the behaviour of rain water which flows down a sloping surface

and (2) that of lateral inflow which pours into a main stream. This runoff mechanism will be similar to that of rain water flow on a road surface and in a road gutter. In this paper, to establish the basic relationship between the rate of inflow and runoff in a stream, the author treats the behaviour of unsteady flows in a uniform and rectangular open channel with the uniform or distributed lateral inflow along a channel as a simplified stream condition. Hydrographs in this simplified condition are easily calculated by the approximate method which utilizes the characteristic equations, in both laminar and turbulent flows, and the hydraulic characters of hydrographs resulting from simulated inflow at a constant rate are investigated in detail.

Moreover, further developed studies on the practical analysis of hydrographs by this approach for existing rivers in Japan will be published before long as a forthcoming paper of this Bulletin.

2. Characteristic Equations for the Flow with Lateral Inflow

For the flow in a rectangular open channel with lateral inflow as shown in Fig. 1, the equation of motion neglecting the vertical acceleration and the equation of continuity are, respectively,[7]

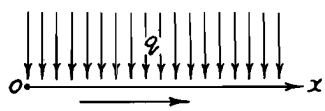

Fig. 1 Scheme of the flow with lateral inflow.

$$\frac{\partial u}{\partial t}+\alpha u\frac{\partial u}{\partial x}-(\alpha-1)\frac{u}{h}\frac{\partial h}{\partial t}+g\cos\theta\frac{\partial h}{\partial x}$$

$$=g\sin\theta-\frac{\tau_0}{\rho R}-\alpha u\frac{q}{h} \qquad \cdots\cdots(1)$$

$$\frac{\partial h}{\partial t}+h\frac{\partial u}{\partial x}+u\frac{\partial h}{\partial x}=q, \qquad \cdots\cdots(2)$$

or

$$\frac{1}{u}\frac{\partial Q}{\partial t}-\frac{Q}{u^2}\frac{\partial u}{\partial t}+\frac{\partial Q}{\partial x}=q, \qquad \cdots\cdots(2)'$$

where q is the rate of lateral inflow per unit width per unit length, Q the discharge rate of flow per unit width, u the mean velocity, h the water depth, R the hydraulic radius, α the momentum correction factor, θ the channel declination, τ_0 the frictional stress on bed, ρ the density of water, g the gravity acceleration, x the distance taking in the downstream direction along the bed, and t the time.

2.1 Strict method

In the same manner in which Escoffier[8] studied the character of the instability of water flow graphically, from Eqs. (1) and (2) the following equations are derived:

$$\left\{\frac{\partial}{\partial t}+(\alpha u+\alpha_1 c)\frac{\partial}{\partial x}\right\}\left\{u+2(\alpha_1-\alpha_2)c\right\}$$

$$=g\sin\theta-\frac{\tau_0}{\rho R}+\frac{q}{h}(\alpha_1 c-\alpha u), \qquad \cdots\cdots(3)$$

$$\left\{\frac{\partial}{\partial t}+(\alpha u-\alpha_1 c)\frac{\partial}{\partial x}\right\}\left\{u-2(\alpha_1+\alpha_2)c\right\}$$

$$=g\sin\theta-\frac{\tau_0}{\rho R}-\frac{q}{h}(\alpha_1 c+\alpha u), \qquad \cdots\cdots(4)$$

where

$$c=\sqrt{gh\cos\theta}, \quad \alpha_1=\sqrt{1+\frac{\alpha(\alpha-1)u^2}{gh\cos\theta}} \text{ and } \alpha_2=\frac{(\alpha-1)u}{\sqrt{gh\cos\theta}}.$$

As in the case of laminar flow, $\alpha = 1.2$ and in the case of turbulent flow, nearly $\alpha = 1.05$, taking the case of $u/\sqrt{gh\cos\theta} = 1$ for example, it becomes respectively $\alpha_1 = 1.11$ and $\alpha_2 = 0.2$ for laminar flow, and $\alpha_1 = 1.026$ and $\alpha_2 = 0.05$ for turbulent flow. For the sake of mathematical simplicity, taking $\alpha = 1$, $\alpha_1 = 1$ and $\alpha_2 = 0$, Eqs. (3) and (4) are written as follows:

$$C_1: \quad \frac{dx}{dt}=u+c,$$

$$\frac{d}{dt}(u+2c)=g\sin\theta-\frac{\tau_0}{\rho R}+\frac{q}{h}(c-u); \qquad \cdots\cdots(3)'$$

$$C_2: \quad \frac{dx}{dt}=u-c,$$

$$\frac{dx}{dt}(u-2c)=g\sin\theta-\frac{\tau_0}{\rho R}-\frac{q}{h}(c+u). \qquad \cdots\cdots(4)'$$

When the initial and boundary conditions are given, u and h at arbitrary values of x and t can be obtained graphically by using the finite difference method and covering over the x-t plane with the above two groupes of characteristic curves C_1 and C_2.[9][10] However, as this strict method is too laborious, the following approximate methods are proposed for the flow in comparatively steep channels.

2.2 Approximate method based on the water depth

(1) *When the lataral inflow rate increases abruptly from* 0 *to* q (Fig. 2).

(a) *Laminar flow.* When the flow is laminar, applying the law of resistance $\tau_0/\rho R = 3\nu u/R^2$ for uniform flow to the unsteady flow in this case approximately, then Eq. (1) is rewritten as follows:

$$u = \frac{R^2 h(g\sin\theta - L)}{3\nu h + \alpha q R^2}, \qquad \cdots\cdots\cdots\cdots(5)$$

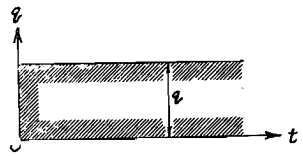

Fig. 2. Relation between lateral inflow rate and time in the case of abrupt increase of inflow rate.

where

$$L = \frac{\partial u}{\partial t} + \alpha u\frac{\partial u}{\partial x} - (\alpha - 1)\frac{u}{h}\frac{\partial h}{\partial t} + g\cos\theta\frac{\partial h}{\partial x}$$

and ν is the kinematic viscosity.

Substituting Eq. (5) into Eq. (2) with the relations $R = Bh/(B+2h)$ and q = constant, the following equation is obtained:

$$\left[\frac{\partial}{\partial t} + \left\{\left(3 - \frac{4R}{B}\right)u - \frac{\alpha u q R^2}{3\nu h + \alpha q R^2}\left(1 - \frac{4R}{B}\right)\right\}\frac{\partial}{\partial x}\right] h = q + \frac{R^2 h^2}{3\nu h + \alpha q R^2}\frac{\partial L}{\partial x}, \qquad \cdots\cdots\cdots\cdots(6)$$

where B is the width of channel.

Now, provided the slope is comparatively steep, so that the flow is nearly uniform, assuming $L = 0$ as the first approximation, Eq. (5) becomes

$$u = \frac{R^2 h g\sin\theta}{3\nu h + \alpha q R^2} \qquad \cdots\cdots\cdots\cdots(5)'$$

Moreover, if $\frac{\partial h}{\partial x} \fallingdotseq 0$, $\frac{\partial u}{\partial x} \fallingdotseq 0$ and $L = \frac{\partial u}{\partial t} - (\alpha - 1)\frac{u}{h}\frac{\partial h}{\partial t}$ are assumed as the second approximation and thereby L is computed from Eq. (5)', the following characteristic equation is derived from Eq. (6):

$$\left.\begin{aligned} \frac{dx}{dt} &= \left(3 - \frac{4R}{B}\right)u - \frac{\alpha u q R^2}{3\nu h + \alpha q R^2}\left(1 - \frac{4R}{B}\right), \\ \frac{dh}{dt} &= q \quad \text{or} \quad h = qt + \text{const.} \end{aligned}\right\} \qquad \cdots\cdots\cdots\cdots(6)'$$

Also, the relationship between u and h is

$$u=\frac{R^2hg\sin\theta\,(3\nu h+\alpha qR^2)}{(3\nu h+\alpha qR^2)^2+\alpha(2-\alpha)\,q^2R^4+3\nu qR^2h\,(3-\alpha-4R/B)}. \qquad \cdots(5)''$$

(b) *Turbulent flow.* In this case, as the friction term, $\tau_0/\rho R=n^2u^2g/R^{4/3}$ is adopted, using Manning's roughness coefficient n. Equating the value of α to unity, Eq. (1) is rewritten

$$u=\sqrt{\left(\frac{qR^{4/3}}{2n^2gh}\right)^2+\frac{R^{4/3}}{n^2g}(g\sin\theta-L)}-\frac{qR^{4/3}}{2n^2gh}. \qquad \cdots\cdots(7)$$

Consequently, the same procedure as in the case of laminar flow yields equations for the second approximation through the first approximation as follows:

$$\left.\begin{aligned}\frac{dx}{dt}&=\left(\frac{5}{3}-\frac{4}{3}\frac{R}{B}\right)u+\frac{uqR^{4/3}}{2n^2ghu+qR^{4/3}}\left(\frac{1}{3}+\frac{4R}{B}\right),\\ \frac{dh}{dt}&=q \quad \text{or} \quad h=qt+\text{const.}\end{aligned}\right\} \qquad \cdots\cdots(8)$$

and

$$u=\sqrt{\left(\frac{5}{3}-\frac{4}{3}\frac{R}{B}\frac{qR^{4/3}}{2n^2gh}\right)+\frac{R^{4/3}}{n^2}\sin\theta-\frac{(2/3+8R/3B)u(qR^{4/3}/2n^2gh)^2}{u+(qR^{4/3}/2n^2gh)}}-\left(\frac{5}{3}-\frac{4R}{3B}\right)\frac{qR^{4/3}}{2n^2gh}. \qquad \cdots\cdots(7)'$$

(2) *When the lateral inflow rate decreases abruptly from q to 0* (Fig. 3).

(a) *Laminar flow.* Substituting $q=0$ into Eqs. (5)'' and (6)', the characteristic equation and the relationship between u and h for laminar flow are obtained as follows:

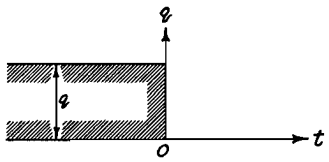

Fig. 3 Relation between lateral inflow rate and time in the case of abrupt decrease of inflow rate.

$$\frac{dx}{dt}=\left(3-\frac{4R}{B}\right)u, \quad h=\text{const.}, \qquad \cdots\cdots(9)$$

and

$$u=\frac{R^2g\sin\theta}{3\nu} \qquad \cdots\cdots(10)$$

(b) *Turbulent flow.* Substituting $q=0$ into Eqs. (7)' and (8), for turbulent flow, it becomes

$$\frac{dx}{dt}=\left(\frac{5}{3}-\frac{4R}{3B}\right)u, \quad h=\text{const.}, \qquad \cdots\cdots(11)$$

and

$$u=\frac{1}{n}R^{2/3}(\sin\theta)^{1/2} \qquad \cdots\cdots\cdots(12)$$

Accordingly, since h and thereby u are constant on the characteristic curves, in both laminar and turbulent flows the characteristic curves are represented by straight lines.

(3) *Transition between two regions under different conditions.*

When the rate of lateral inflow q is constant in each definite time interval, and also q or the slope and roughness of bed are uniform, in each definite reach along the stream, for each region on the x-t plane the above relationships can be applied. However, because of the difference of the relations between u and h in each region, water depth or discharge rate obtained from Eqs. (5)′′, (7)′, (10) and (12) becomes discontinuous on the boundary of each region. Therefore, it is necessary to consider the transition between two different regions.

(a) *Transition due to change of inflow rate with respect to time.* For example, from Eqs. (7)′ and (12) representing the relations between u and h for turbulent flow in the cases of a finite inflow rate q and $q=0$ respectively, it is understood that the mean velocity in the latter case is larger than that in the former for the same depth. Consequently, if water depth is continuous at an instant of stop of inflow supply, $t=0$, mean velocity and discharge rate increase abruptly and become discontinuous at this moment. On the other hand, if mean velocity and discharge rate are continuous, water depth needs to decrease abruptly. The phenomenon of a temporal increase of discharge rate is shown in some hydrographs for a paved plot obtained by Izzard and Augustine.[2] However, it seems to be irrational that the relation between u and h changes discontinuously from that in the case of finite inflow rate q to that in the case of $q=0$. Consequently, the transition between these two conditions should be introduced.

Now, let the inflow rate in this region not be restricted to $q=0$, but be assumed $q=q_3$ generally. It is also assumed that this transition region is between $t=0$ and $t=t_3$ as shown in Fig. 4 and the points ①, ② and ③ are near each other. Then the following finite difference expressions are obtained from Eqs. (3)′ and (4)′:

$$\frac{x_3-x_1}{t_3}=\frac{1}{2}(u_1+u_3+c_1+c_3), \qquad \cdots\cdots\cdots(13)$$

$$u_3-u_1+2(c_3-c_1)+\frac{1}{2}\left\{\left(\frac{\tau_0}{\rho R}\right)_1-g\sin\theta\right\}t_3+\frac{1}{2}\left\{\left(\frac{\tau_0}{\rho R}\right)_3-g\sin\theta\right\}t_3$$
$$-\frac{2gq_3\cos\theta}{(c_1+c_3)^2}\left\{c_1+c_3-(u_1+u_3)\right\}t_3=0; \quad \cdots\cdots(13)'$$

$$\frac{x_3-x_2}{t_3}=\frac{1}{2}(u_2+u_3-c_2-c_3), \quad \cdots\cdots(14)$$

$$u_3-u_2-2(c_3-c_2)+\frac{1}{2}\left\{\left(\frac{\tau_0}{\rho R}\right)_2-g\sin\theta\right\}t_3+\frac{1}{2}\left\{\left(\frac{\tau_0}{\rho R}\right)_3-g\sin\theta\right\}t_3$$
$$+\frac{2gq_3\cos\theta}{(c_1+c_3)^2}\left\{c_2+c_3+(u_2+u_3)\right\}t_3=0. \quad \cdots\cdots(14)'$$

Moreover, as the point (x_1, t_1) is near the point (x_2, t_2), equating approximately

$$u_1=u_2 \quad \text{and} \quad c_1=c_2, \quad \cdots\cdots(15)$$

the following relation is derived from Eqs. (13)′ and (14)′:

$$c_3^2=c_1^2+gq_3\cos\theta\, t, \quad \cdots\cdots(16)$$

or

$$h_3=h_1+q_3t. \quad \cdots\cdots(16)'$$

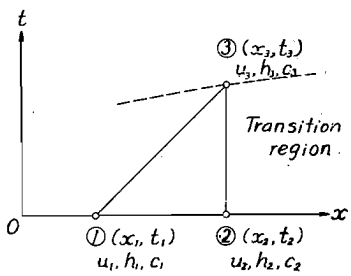

Fig. 4 Transition region due to change of condition with respect to time.

Also, from this relation and Eq. (13)′,

$$\frac{2(u_3-u_1)}{t_3}+\left\{\left(\frac{\tau_0}{\rho R}\right)_1+\left(\frac{\tau_0}{\rho R}\right)_3-2g\sin\theta\right\}$$
$$+\frac{4(c_3-c_1)(u_1+u_3)}{(c_1+c_3)t_3}=0, \quad \cdots\cdots(17)$$

and from Eq. (13),

$$x_3=\frac{t_3}{2}(u_1+u_3+c_1+c_3)+x_1 \quad \cdots\cdots(18)$$

are obtained respectively. If $q_3=0$, Eqs. (16)′, (17) and (18) are expressed as follows:

$$h_3=h_1, \quad \cdots\cdots(16)''$$

$$t_3=\frac{2(u_3-u_1)}{g\sin\theta-(\tau_0/\rho R)_1}, \quad \cdots\cdots(17)'$$

$$x_3=\frac{t_3}{2}\left(u_1+u_3+2\sqrt{gh_1\cos\theta}\right)+x_1. \quad \cdots\cdots(18)'$$

If the point ③ is fixed using the above equations, thereafter the equations put $q=q_3$ in Eqs. (5)″ and (6)′ or Eqs. (7)′ and (8) are applied. In the

transition region, it may be assumed that the characteristic curve $\overline{①\ ③}$ is straight and on this line the same relation as Eq. (16)′

$$h=h_1+q_3t \qquad \cdots\cdots\cdots\cdots\cdots (16)''$$

is applied, and that mean velocity and discharge rate change linearly from u_1 and Q_1 to u_3 and Q_3, respectively.

(b) *Transition due to change of inflow rate and channel conditions with respect to distance.* The transition region in this case is formed between $x = 0$ and $x = x_3$ as shown in Fig. 5. In such a manner as the transition with respect to time, let it be assumed that the points ①, ② and ③ are near each other. Then the following finite difference expression are obtained:

$$\frac{x_3}{t_3-t_1}=\frac{1}{2}(u_1+u_3+c_1+c_3), \qquad \cdots\cdots\cdots\cdots\cdots (19)$$

$$u_3-u_1+2(c_3-c_1)+\frac{1}{2}\left\{\left(\frac{\tau_0}{\rho R}\right)_1-g\sin\theta_3\right\}(t_3-t_1)$$
$$+\frac{1}{2}\left\{\left(\frac{\tau_0}{\rho R}\right)_3-g\sin\theta_3\right\}(t_3-t_1)$$
$$-\frac{2gq_3\cos\theta_3}{(c_1+c_3)^2}\left\{c_1+c_3-(u_1+u_3)\right\}(t_3-t_1)=0\,; \qquad \cdots\cdots\cdots\cdots\cdots (19)'$$

$$\frac{x_3}{t_3-t_2}=\frac{1}{2}(u_2+u_3-c_2-c_3), \qquad \cdots\cdots\cdots\cdots\cdots (20)$$

$$u_3-u_2-2(c_3-c_2)+\frac{1}{2}\left\{\left(\frac{\tau_0}{\rho R}\right)_2-g\sin\theta_3\right\}(t_3-t_2)$$
$$+\frac{1}{2}\left\{\left(\frac{\tau_0}{\rho R}\right)_3-g\sin\theta_3\right\}(t_3-t_2)$$
$$+\frac{2gq_3\cos\theta_3}{(c_2+c_3)^2}\left\{c_2+c_3+(u_2+u_3)\right\}(t_3-t_2)=0. \qquad \cdots\cdots\cdots\cdots\cdots (20)'$$

Moreover, it is assumed that the following relation

$$u_3h_3=u_1h_1+q_3x_3, \qquad \cdots\cdots\cdots (21)$$

or

$$Q_3=Q_1+q_3x_3, \qquad \cdots\cdots\cdots (21)'$$

is held between the points ① and ③. Although the assumption of Eq. (21) or (21)′ couldn't be completely approved, the results computed with this assumption in the approximate method based upon the discharge rate described in the next section were confirmed

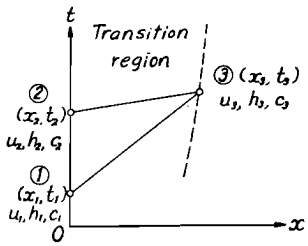

Fig. 5 Transition region due to change of condition with respect to distance.

to show very good agreement compared with those obtained by Eqs. (19)~(20)′ for some examples. Also, from Eqs. (19) and (19)′

$$\frac{\{u_3-u_1+2(c_3-c_1)\}\{u_1+u_3+c_1+c_3\}}{x_3}+\left\{\left(\frac{\tau_0}{\rho R}\right)_1+\left(\frac{\tau_0}{\rho R}\right)_3-2g\sin\theta_3\right\}$$

$$-\frac{4gq_3\cos\theta_3(c_2+c_3-u_2-u_3)}{(c_1+c_3)^2}=0 \qquad \cdots\cdots(22)$$

is derived, and Eq. (19) is written

$$t_3=\frac{2x_3}{u_1+u_3+c_1+c_3}+t_1. \qquad \cdots\cdots(23)$$

When $q_3=0$, u_3 and c_3 are obtained from Eq. (10) or (12) as $Q_3=Q_1$ from Eq. (21)′. Consequently, x_3 is directly computed, and t_3 is obtained from Eq. (23). However, when $q\neq 0$, x_3 must be obtained by the cut-and-try procedure.

2.3 Approximate method based on the dischange rate.

(1) *When the lateral inflow rate increases abruptly from* 0 *to* q (Fig. 2).

(a) *Laminar flow.* Considering comparatively steep channels as in the case of the method based on the water depth and using Eq. (5)′ as the first approximation, yields

$$\frac{du}{dt}=\frac{u}{Q}\left\{\left(2-\frac{4R}{B}\right)u-\frac{(1-4R/B)\,\alpha uqR^2}{3\nu h+aqR^2}\right\}\left(q-\frac{\partial Q}{\partial x}\right),$$

and substituting this equation into Eq. (2)′, the following equation is obtained:

$$\left[-\frac{\partial}{\partial t}+\left\{\left(3-\frac{4R}{B}\right)u-\frac{(1-4R/B)\,\alpha uqR^2}{3\nu h+aqR^2}\right\}\frac{\partial}{\partial x}\right]Q$$

$$=q\left\{\left(3-\frac{4R}{B}\right)u-\frac{(1-4R/B)\,\alpha uqR^2}{3\nu h+aqR^2}\right\}. \qquad \cdots\cdots(24)$$

This equation is also expressed as the characteristic equations

$$\left.\begin{aligned}\frac{dx}{dt}&=\left(3-\frac{4R}{B}\right)u-\frac{(1-4R/B)\,\alpha uqR^2}{3\nu h+aqR^2},\\ \frac{dQ}{dt}&=q\left\{\left(3-\frac{4R}{B}\right)u-\frac{(1-4R/B)\,\alpha uqR^2}{3\nu h+aqR^2}\right\},\end{aligned}\right\} \qquad \cdots\cdots(24)'$$

that is $$\frac{dQ}{dx}=q.$$

For the relation between u and h, Eq. (5)″ is used as the second approxi-

mation.

(b) *Turbulent flow.* If the law of resistance of Manning's type is used, by the same procedure as in the case of laminar flow the following characteristic equations are derived:

$$\left.\begin{aligned}\frac{dx}{dt}&=\left(\frac{5}{3}-\frac{4R}{3B}\right)u+\frac{(1/3+4R/3B)\,uqR^{4/3}}{2n^2ghu+qR^{4/3}},\\ \frac{dQ}{dt}&=q\left(\frac{5}{3}-\frac{4R}{3B}\right)u+\frac{(1/3+4R/3B)\,uqR^{4/3}}{2n^2ghu+qR^{4/3}},\end{aligned}\right\}\quad\cdots\cdots\cdots(25)$$

that is

$$\frac{dQ}{dx}=q$$

For the relation between u and h, Eq. (7)′ is also used.

(2) *When the lateral inflow rate decreases abruptly from q to* 0 (Fig. 3).

Along each characteristic curve in the transition region, the water depth h does not change, but the discharge rate Q changes. However, when t_3 and x_3 are computed as in the previously described procedure and the point ③ in Fig. 4 is fixed, thereafter the following characteristic equations are applied:

Laminar flow:

$$\left.\begin{aligned}\frac{dx}{dt}&=\left(3-\frac{4R}{B}\right)u,\\ Q&=\text{const.}\end{aligned}\right\}\quad\cdots\cdots\cdots\cdots\cdots(26)$$

Turbulent flow:

$$\left.\begin{aligned}\frac{dx}{dt}&=\left(\frac{5}{3}-\frac{4R}{3B}\right)u,\\ Q&=\text{const.}\end{aligned}\right\}\quad\cdots\cdots\cdots\cdots\cdots(27)$$

3. Some Examples of Numerical Computations

Some numerical computations by the above described approximate methods were conducted for the following certain definite numerical values of the channel dimensions and conditions:

(A) Channel width $B=19.6$ cm, total length $=24$ m, Manning coefficient $n=0.009$ (m-s unit), $\sin\theta=0.015$, kinematic viscosity of water $\nu=0.01\text{cm}^2/\text{s}$, and $q=1/12=0.0833$ cm/s having the constant value along the channel.

(B) Channel width, total length, Manning coefficient and kinematic viscosity are the same values as in (A), and both $\sin\theta=0.020$, 0.015 and 0.010, and $q=0.1080$, 0.0638 and 0.800 cm/s in each reach of channel $x=0-8$ m,

8 - 16 m and 16 - 24 m respectively.

Under these conditions, hydrographs resulting from the lateral inflows for the following cases were computed:

(a) The lateral inflow rate increases abruptly from 0 to q simultaneously along the channel.

(b) The lateral inflow rate decreases abruptly from q to 0 simultaneously along the channel.

(c) The lateral inflow is given only for the time durations, $T=10$, 20, 30 and 40 sec.

(1) *When the lateral inflow rate increases abruptly from* 0 *to* q *simultaneously along the channel.*

The velocity-depth and discharge rate-depth relations for $q=0.0833$ cm/s and $q=0$ obtained from Eqs. (5)'' and (7)' and Eqs. (10) and (12) respectively are shown in Fig. 6. In this figure, it is obviously seen that both values of velocity and discharge rate in the case of $q=0$ are larger than those in the case of $q=0.0833$ cm/s at all values of depth.

When the values of Reynolds number $R_e=uR/\nu$ are less than 500 or more than 1500, flows are regarded to be laminar or turbulent, respectively[11], and therefore the behaviour of prescribed equations is considered to show the characteristics for each flow region. In the transition from laminar to turbulent flow, $1500>R_e>500$, the velocity- and discharge rate-depth re-

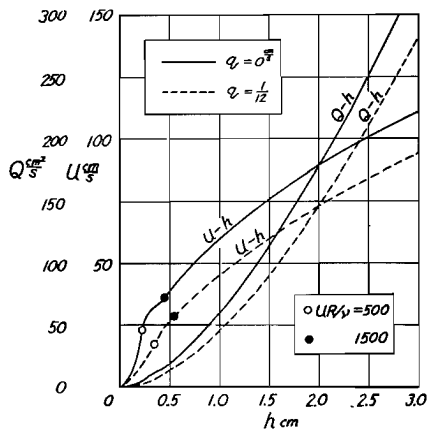

Fig. 6 Velocity-depth and discharge rate-depth relations for $q=0$ and $q=0.833$ cm/s.

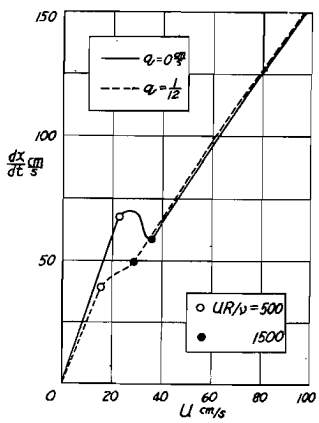

Fig. 7 Relations between u and dx/dt for $q=0$ and $q=0.0833$cm/s.

lations are expressed by curves connecting smoothly curves of both laminar and turbulent flows together.

Fig. 7 shows the relation between u and dx/dt obtained from Eqs. (6)′, (8), (9) and (11) and a set of curves shown in Fig. 6. The characteristic curves can be computed by using Eqs. (6)′, (8), (24)′ and (25) and relations shown in Figs. 6 and 7. The characteristic curves obtained for the channel condition (A) are shown in Fig. 8. The results denoted as the strict method for $\alpha=1$ in this figure are those computed by the finite difference method from Eqs. (3)′ and (4)′, using $\tau_0/\rho R=3\nu u/R^2$ for laminar and $\tau_0/\rho R=n^2u^2g/R^{1/3}$ for turbulent flow. As the boundary condition, hereon, the source of supply of water consists of only the lateral inflow and the inflow from the upper end of the channel is not given. That is, hydraulically speaking, as $h=0$ at $x=0$, the flow becomes steady along the characteristic curve C_0 starting from the origin. Hence, the curve C_0 forms the boundary between the steady and unsteady regions as seen in Fig. 8. Provided x is constant, dx/dt is also constant. Thus the characteristic curves in the steady region are drawn by moving the curve C_0 parallel to the t-axis. Since u, h and Q are zero along the channel at $t=0$, as the initial condition, in the unsteady region the values of dx/dt are the

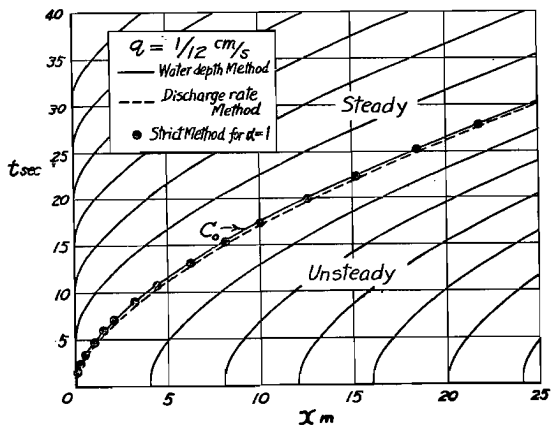

Fig. 8 Characteristic curves in the channel condition (A) and the inflow condition (a).

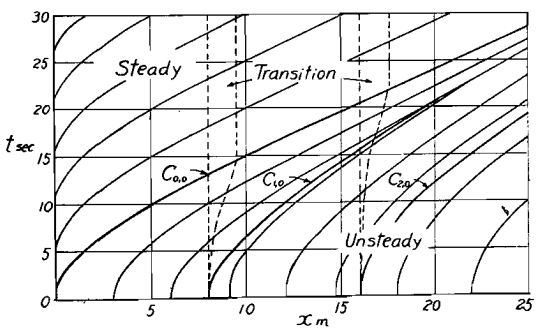

Fig. 9 Characteristic curves in the channal condition (B) and the inflow condition (a).

same in all values of x at a given instant t. Consequently, the characteristic curves in the unsteady region are drawn by moving the curve C_0 parallel to the x-axis. Hence the depth h increases linearly to the time t, in the unsteady region, because of the relation $h=qt$ along the characteristic curves.

The characteristic curves obtained for the channel condition (B) is shown in Fig. 9. In this figure, each set of curves in three unsteady regions between the x-axis and $C_{0,0}$, $C_{1,0}$ and $C_{2,0}$, starting from the upstream end of each reach with different flow condition can be drawn until arriving at the transition regions, by moving $C_{0,0}$, $C_{1,0}$ and $C_{2,0}$ parallel to the x-axis, respectively. And the transition regions are those caused by the changes of lateral inflow rate and channel conditions with respect to distance.

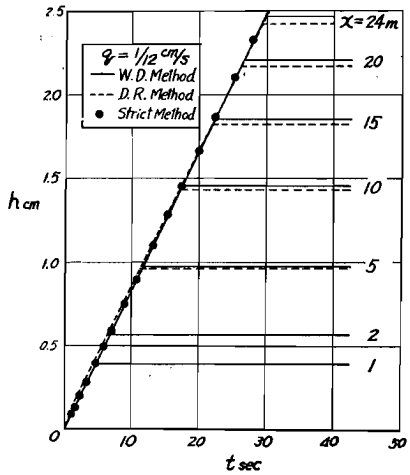

Fig. 10 Variation of water depth as a function of time in the channel condition (A) and the inflow condition (a).

The behaviour of the variations of water depth, mean velocity and discharge rate as a function of time for the channel condition (A) is shown

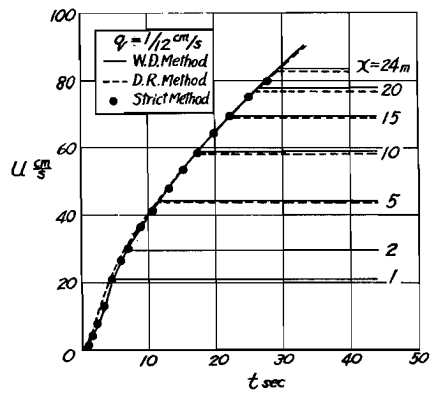

Fig. 11 Variation of mean velocity as a function of time in the channel condition (A) and the inflow condition (a).

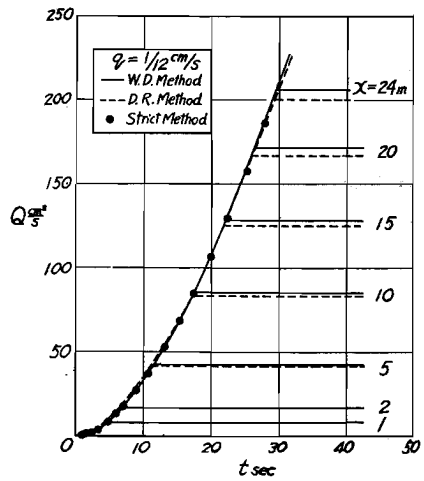

Fig 12 Variation of discharge rate as a function of time in the channel condition (A) and the inflow condition (a).

in Figs. 10, 11 and 12.

In these figures, the lapsed time until the flow becomes steady for any point is obtained from Fig. 8.

For the channel condition (A), the behaviour of the variation of water surface profile as a function of time is shown in Fig. 13.

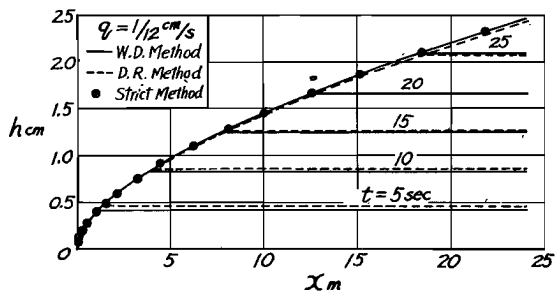

Fig. 13 Variation of water surface profile in the channel condition (A) and the inflow condition (a).

As seen in the above presented figures, both results by methods based on the water depth and on the discharge rate coincide well with a maximum difference of about 2 %. Also, the results by the strict method for $\alpha=1$ show good agreement compared with those by two approximate methods. This agreement may be due to the fact that in the unsteady region, in which the disturbance of upstream end does not reach anywhere, the second approximation obtained by putting $\partial h/\partial x=0$ and $\partial u/\partial x=0$ is not approximate but quite rigorous.

The behaviour of the variation of water surface profile obtained by the water depth method for the channel condition (B) is shown in Fig. 14. In this figure, it is seen that the flow in this case becomes gradually steady, appearing rather complex behaviour of the variation of water surface profile as compared with the case of channel condition (A).

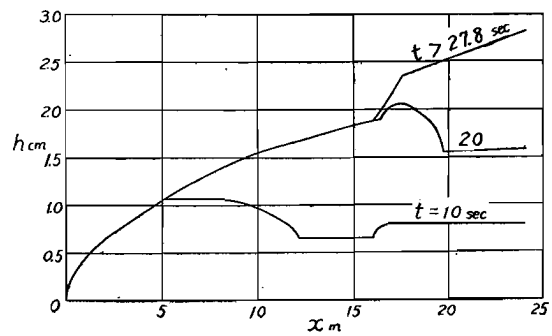

Fig. 14 Variation of water surface profile in the channel condition (B) and the inflow condition (a).

(2) *When the lateral inflow rate decreases abruptly from q to 0 along the channel.*

Fig. 15 shows the straight characteristics obtained by the water depth

method for the channel condition (A). As the initial condition at $t=0$, that is, when the lateral supply of water is stopped, the water depth h for any point along the channel is determined from Fig. 13. Hence u_1 and u_3 in Eq. (17)′ are calculated as particular values of velocity corresponding to water depth h obtained for both cases of $q=$ 0.0833 cm/s and $q=0$. Furthermore, t_3 is computed from Eq. (17)′ by using the above obtained u_1 and u_3, and x_3 is also calculated from Eq. (18)′. Consequently the straight characteristics in the transition region can be drawn. In this case, the transition means that caused by the change of inflow rate as a function of time. Partly the point ③, (x_3, t_3), was calculated by the strict method based upon Eqs. (13), (13)′, (14) and (14)′, resulting in the conclusion that the approximate method by Eq. (15) showed a good agreement with the strict method, and also the relation $h_3=h_1$ and the assumption of straight line for $\overline{①\ ③}$ were considered to be satisfactory. Since, starting from the point ③, (x_3, t_3), the straight characteristics given by Eqs. (9) and (11) can be drawn. the depth-time relations for any point are also obtained from this diagram of characteristics, and moreover velocity-and discharge rate-time relations are also calculated. These results are shown in the inflow condition (c) described below.

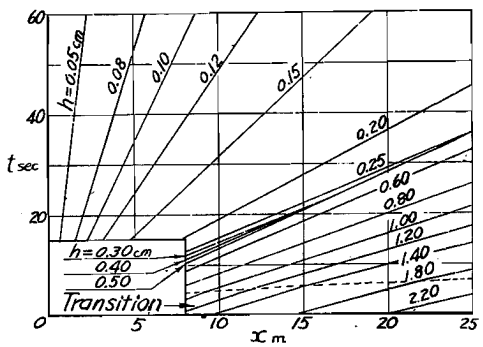

Fig. 15 Straight characteristics in the channel condition (A) and the inflow condition (b).

The straight characteristics for the channel condition (B) obtained by the water depth method are shown in Fig. 16, in which at $t=0$, that is, when the lateral supply is stopped, the water depths along the channel are determined from Fig. 14. In this case, the two kinds of transition

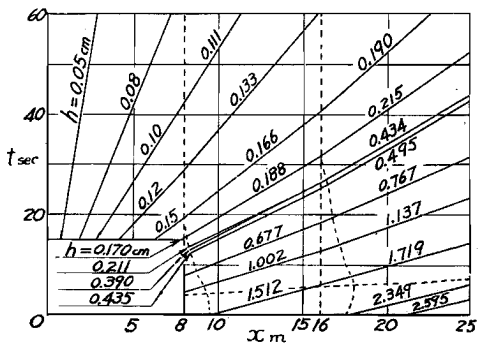

Fig. 16. Straight characteristics in the channel condition (B) and the inflow condition (b).

region caused by the changes of lateral inflow rate and channel conditions as functions of time and distance appear in the x–t plane, namely Fig. 16.

(3) *When the lateral inflow is given only during a definite time duration.*

As shown in Fig. 17, when the lateral inflow at a constant rate is supplied only during the time interval T before $t=0$, the required hydrographs can be obtained by combining the results in both inflow conditions (a) and (b). Until the lateral supply is stopped, the hydrographs show the same behaviour as in those described in Article (1), but, hereafter at any point in the steady region at $t=0$, water depth, mean velocity and discharge rate begin to decrease together at the instant of stop of lateral supply. On the other hand, for any point in the unsteady region where the disturbance of upstream end does not yet reach at $t=0$, the water depth upward from a given point exerts influence on the change of water depth at that point. In channel condition (A), for example, as the water depth at a point in the unsteady re-

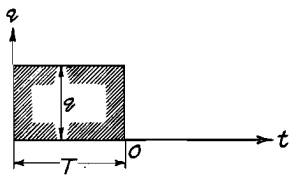

Fig. 17. Relation between lateral inflow rate and time in the inflow condition (c).

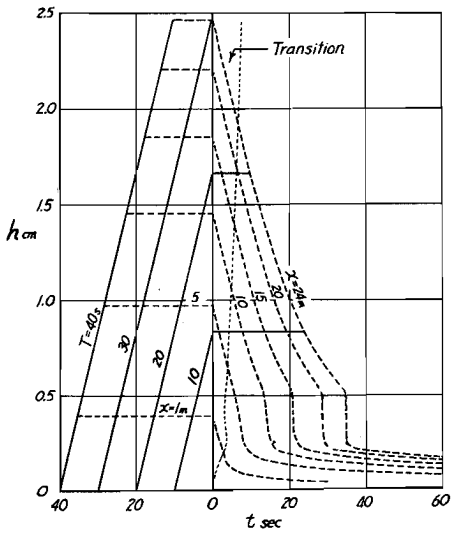

Fig. 18 Computed hydrographs for water depth in the channel condition (A) and the inflow condition (c).

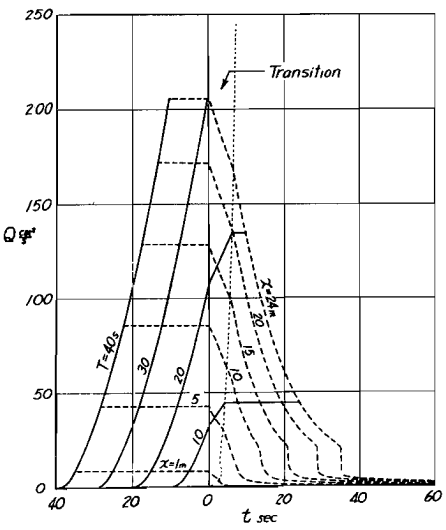

Fig. 19 Computed runoff hydrographs in the channel condition (A) and the inflow condition (c).

gion is uniform as shown in Fig. 13, so the water depth does not change until the arrival of the distrubance of upstream end at this point, but immediately after the arrival of this disturbance it begins to decrease. In the channel condition (B), however, as the behaviour of water surface profile appears rather complex at all points in the unsteady region as shown in Fig. 14, even until the arrival of the disturbance of upstream end the water depth is not constant, but changes, not as in the channel condition (A). Figs. 18 and 19 show the hydrographs for water depth and discharge rate at each point in the channel condition (A), drawn for various parametric values of duration time of inflow T by taking the time axis as shown in Fig. 17. These are both hydrographs obtained by the approximate water depth method. It is seen from these figures that in the cases of $T=30$ sec. and 40 sec. the flows become steady overall along the channel before the lateral supply is stopped. As shown in Fig. 7, in the case of $q=0$, there exists a condition that the dx/dt in laminar flow is larger than that in turbulent flow, even though the velocity is smaller. Accordingly, some straight characteristics in the vicinity of transition region between both regions of flow intersect eact other, so that the abruptly decreasing parts of water depth and discharge rate appear as seen in Figs. 18 and 19, and this phenomenon becomes more remarkable in downstream reaches.

In the channel condition (B), the hydrographs for various cases of inflow condition cannot be drawn together as in Figs. 18 and 19.

With respect to the variation of water surface profile as a function of time, the behaviour for the rising limb of hydrograph was already shown in Figs. 13 and 14. On the other hand, the variation of water surface profile for the descending limb can be drawn by using the characteristics in the inflow condition (b) given in Figs. 15 and 16. As an example, the behaviour of the variation of water surface profile in the channel condition (A) is shown in Fig. 20. This figure also shows the variation in the inflow condition (c).

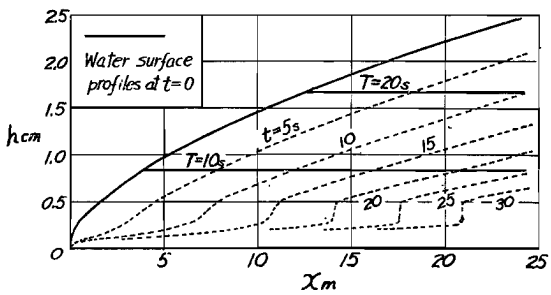

Fig. 20 Variation of water surface in the channel condition (A) and the inflow condition (c).

4. Experiments

In order to ascertain the validity of results of calculation presented above, a course of experiments was performed in detail at the Hydraulic Lahoratory, Kyoto University.

4.1 Apparatus and procedure

The exprerimental flume has a rectangular cross section of 19.6 cm width and 9 cm effective depth. Its total length is 24 m and the flume is made of aluminum. The flume slope is set at the same inclination as in the computed examples, that is uniform along the flume and $\sin\theta=0.015$ in the channel condition (A), and $\sin\theta=0.020$, 0.015 and 0.010 for $x=0-8$ m, 8 - 16 m and 16 - 24 m respectively in the channel condition (B).

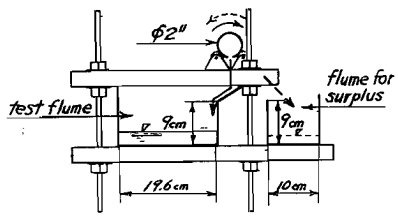

Fig. 21. Mechanism of lateral supply of water into the experimental flume.

The inflow water was supplied by a rotative iron pipe of 2 in. diameter having many small holes of 2.5 - 3.2 mm diameter, from which water jets and pours into the experimental flume as shown in Fig.2 1.

Simultaneous supply and stoppage overall along the flume are made by the rotation of the pipe. In channel condition (A), these small holes were opened at intervals of 10 cm, so that the lateral supply of water was as uniform as possible along the flume. In the channel condition (B), on the other hand, the water supply was so adjusted as to become $q=0.1080$ cm/s, 0.0638 cm/s and 0.0800 cm/s by the pertinent closure of holes, for the flume reaches $x=0-8$ m, 8 - 16 m and 16 - 24 m respectively. At one side of the test flume, a drain flume of 10 cm width, 9 cm depth and 24 m length was placed as shown in Fig. 21, and water jetting from these small holes was supplied into this flume by the rotation of pipe as the condition of $q=0$.

Measurements of water depth were made at points, $x=10$ m, 15 m, 20 m and 24 m by the electric self-recording water gauges, because of the quick change of water level. To measure the change of discharge rate, water level of the weir set to a box (40 cm by 40 cm square cross section and 45 cm depth) beneath the downstream end of the flume was first recorded in the same manner as mentioned above. However, as it was difficult to obtain the change of discharge rate accurately, owing to the effect of water storage in the box, this measure-

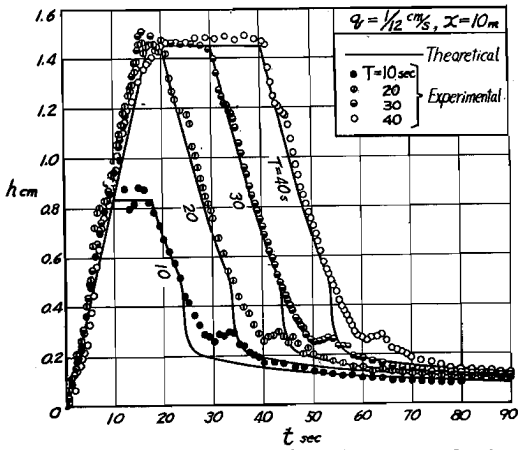

Fig. 22(a) Hydrographs for the water depth obtained by the experiments and computations at $x=10$ m in the channel condition (A).

ment was abandoned and then the accumulating method was adopted. That is,the accumulated discharge was measured by recording the water level in another box (50 cm by 60 cm rectangular cross section and 60 cm depth) that is capable of storing the total discharge, and from this record the rate of change of discharge was calculated.

4.2 Results and considerations

Figs. 22 (a), (b), (c) and 23 (a), (b) show some examples of the results of experiments and theoretical computations in the channel conditions (A) and (B), respectively. In these figures, the origin of time-axis was taken at the initiation of lateral supply of water, not as in Figs. 18 and 19. From Figs. 22 and 23, it is understood that:

(1) The computed results by the approximate method proposed by the author are in good agreement with

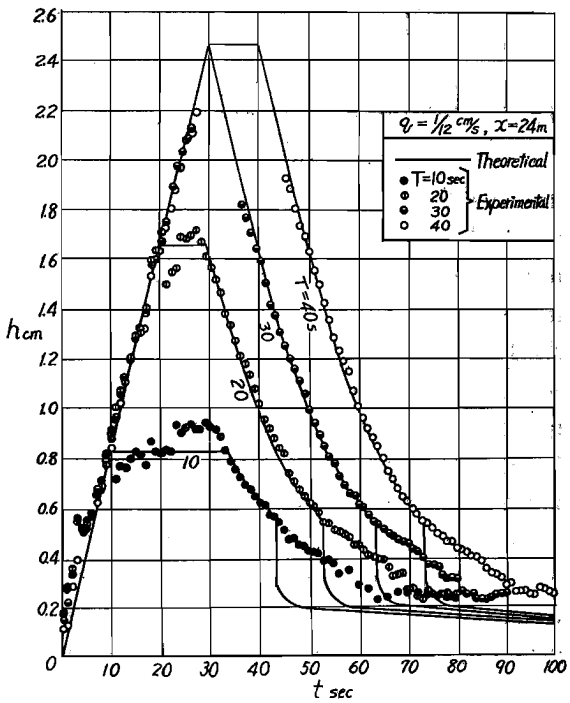

Fig. 22(b) Hydrographs for the water depth obtained by the experiments and computations at $x=24$ m in the channel condition (A).

the experimental values. Though, in the channel condition (B), as shown in Figs. 23(a) and (b), there are some parts where the experimental values are somewhat out of the computed curves, it may be due to the reason that the uniformity of lateral inflow rate q at each reach of the flume was considered to be unsatisfactory.

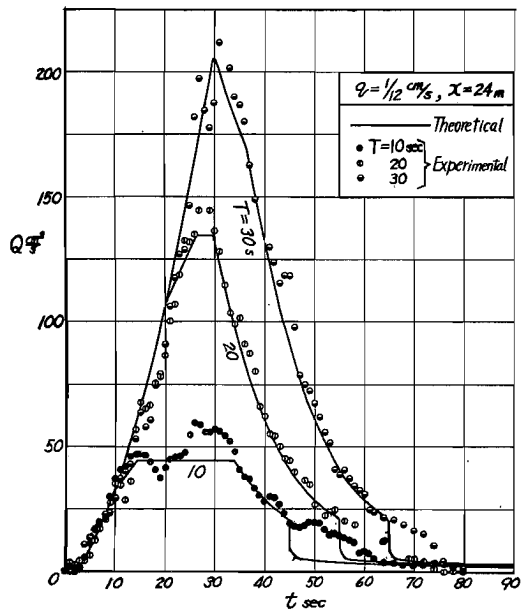

Fig. 22(c) Hydrographs for the discharge rate obtained by the experiments and computations at $x=24$ m in the channel condition (A).

(2) In both cases of $T=$ 10 sec. and 20 sec., whenever the lateral inflow rate becomes 0, the discharge rate and the water depth will not begin to decrease, and, on the contrary, the former increases.

(3) The phenomenon that the water depth and discharge rate decrease suddenly at the transition of descending limb of hydrographs from turbulent to laminar flow is not so remarkable in the experiments as in the theoretical results, but yet appears later than the theoretically computed hydrographs. This may perhaps be due to the fact that the critical Reynolds Numbers become smaller than those used in the computations because of any cause like the irregularity of flume bottom or disturbance.

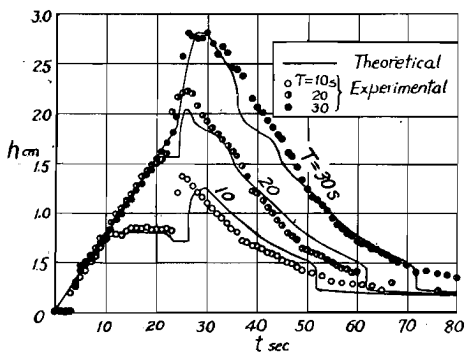

Fig. 23(a) Hydrographs for the water depth obtained by the experiments and computations at $x=24$ m in the channel condition (B).

(4) Although the experimental results of discharge rate are plotted more scattered than those of water depth, it is rather difficult to obtain

more accurate results by the accumulating method.

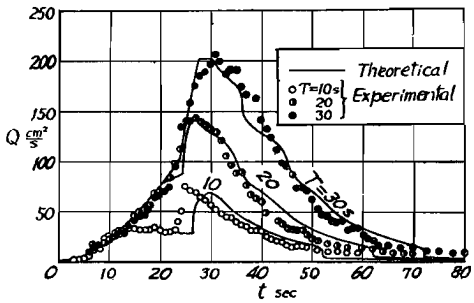

Fig. 23 (b) Hydrographs for the discharge rate obtained by the experiments and computations at $x=$ 24 m in the channel condition (B).

5. Approximate Method by Characteristics for Calculation of Unsteady Flows in Channels of Any Cross-sectional Shape with Lateral Inflow

For the purpose of runoff analysis in an existing river, it is necessary to develop the author's method by characteristics for open channels of any cross-sectional shape.

In the case of any cross-sectional channel, the equations of motion and continuity are, instead of Eqs. (1), (2) and (2)′, expressed as[7]

$$\frac{\partial u}{\partial t}+\alpha u\frac{\partial u}{\partial x}-(\alpha-1)\frac{u}{A}\frac{\partial h}{\partial t}+g\cos\theta\frac{\partial h}{\partial x}$$
$$=g\sin\theta-\frac{\tau_0}{\rho R}-\alpha u\frac{q^*}{A}, \qquad \cdots\cdots(28)$$

$$\frac{\partial A}{\partial t}+A\frac{\partial u}{\partial x}+u\frac{\partial A}{\partial x}=q^*. \qquad \cdots\cdots(29)$$

or

$$\frac{1}{u}\frac{\partial Q^*}{\partial t}-\frac{Q^*}{u^2}\frac{\partial u}{\partial t}+\frac{\partial Q^*}{\partial x}=q^*. \qquad \cdots\cdots(29)'$$

where q^* is the rate of lateral inflow per unit length, Q^* the discharge rate of flow in the total cross-section of channel, and A the cross-sectional area of flowing water.

Introducing the characteristic equation of the second approximation from Eqs. (28),(29) and (29)′ by the same procedure as in the case of the rectangular channel described previously, the following expressions are obtained for turbulent flow:

$$\left.\begin{aligned}\frac{dx}{dt}&=\left(1+\frac{2}{3\beta}\right)u+\frac{(1-2/3\beta)\,uq^*R^{4/3}}{2n^2gAu+q^*R^{4/3}},\\ \frac{dA}{dt}&=q^*,\\ \frac{dQ^*}{dx}&=q^*,\end{aligned}\right\}\qquad\cdots\cdots(30)$$

or

and the relation between u and A is

$$u=\sqrt{\left\{\left(1+\frac{2}{3\beta}\right)\frac{q^*R^{4/3}}{2n^2gA}\right\}+\frac{R^{4/3}\sin\theta}{n^2}}-\frac{2\{1-(2/3\beta)\}u'(q^*R^{4/3}/2n^2gA)}{u'+(q^*R^{4/3}/2n^2gA)}$$
$$-\left(1+\frac{2}{3\beta}\right)\frac{q^*R^{4/3}}{2n^2gA}\,.\qquad\cdots\cdots(31)$$

where

$$u'=\sqrt{\left\{\left(1+\frac{2}{3\beta}\right)\frac{q^*R^{4/3}}{2n^2gA}\right\}^2+\frac{R^{4/3}\sin\theta}{n^2}}-\left(1+\frac{2}{3\beta}\right)\frac{q^*R^{4/3}}{2n^2gA}\,.$$

and β the coefficient which is included in the relation put as

$$\frac{\partial R}{\partial x}=\frac{\partial R}{\partial A}\cdot\frac{\partial A}{\partial x}=\frac{R}{\beta A}\cdot\frac{\partial A}{\partial x}$$

The value of this coefficient is generally between unity for rectangular and wide channel and two for triangular channel.

When there is no lateral inflow, moreover, putting $q^*=0$ in the above equations yields

$$\left.\begin{aligned}\frac{dx}{dt}&=\left(1+\frac{2}{3\beta}\right)u\,,\\ A&=\text{ const.}\quad\text{or}\quad Q^*=\text{ const.}\end{aligned}\right\}\qquad\cdots\cdots(32)$$

and Eq. (31) becomes Manning's formula

$$u=\frac{1}{n}R^{2/3}(\sin\theta)^{1/2}\qquad\cdots\cdots(33)$$

In applying this method to runoff analysis in an existing river, the value of q^* is usually so small that, as the relation between u and A, Eq. (33) can be used satisfactorily instead of Eq. (31). In this case, therefore, since the relation between u and A becomes to be independent of the value of q^*, the transition region as a function of time vanishes, and only that caused by the abrupt change of q^* and the channel conditions along a stream remains.

This method by the characteristic approach was applied to the hydraulic analysis of the storm runoff which damaged the basin of River Daido over a drainage

area of 189.1 km^2 and of a 38.9 km length of main water course in September, 1953 by Mr. T. Sueishi under the author's instruction.[12] The results were very successful, and then it was approved that this runoff analysis method established by the knowledge of advanced hydraulics in more recent years would be an effective tool for the analysis of runoff estimation in a mountainous district. Practical work on these problems will be reported in a forthcoming paper.

Conclusion

An approximate method for calculation of unsteady flow in open channels with lateral inflow, especially which increases or decreases abruptly, using the characteristics, was proposed. The calculated results by this method and those obtained by the experiments in the same conditions were compared, and it was seen that both results were in good agreement. When, therefore, the channel slope is comparatively steep and hence the flow is nearly uniform, such an approximation as described previously may be permitted satisfactorily.

Moreover, this approximate method by characteristics was developed for unsteady flow in open channels of any cross-sectional shape, and it was noted that the proposed method would be applicable to the hydraulic analysis of runoff estimation in actual rivers.

Among the results obtained in this investigation, the interesting points are summarized as follows:

(1) When the lateral inflow rate changes abruptly from 0 to constant rate q, if q is uniform along the channel, the water depth increases linearly according to the relation $h = qt$.

(2) When the lateral inflow rate changes abruptly from q to 0, the water depth and discharge rate at the point where the flow is already in a steady state begin to decrease suddenly. But at the point in an unsteady state, these phenomena don't occur at once; on the contrary the discharge rate increases in the transition region.

(3) It is found theoretically that when the water depth and the discharge rate decrease, these values drop suddenly near the transition from turbulent to laminar. This phenomenon is not so clear in the experiments, but can be observed to some extent.

(4) This method by characteristics is developed for any cross-sectional channel and applicable to runoff analysis in a comparatively steep river.

Acknowledgments

The author is greatly indebted to Prof. Tojiro Ishihara for his constant instruction in performing this study. Thanks are also due to Mr. T. Sueishi, by whom the experiments and the computations were conducted under the author's supervision, and to Assist. Prof. Y. Iwasa who assisted in the preparation of this paper.

References

1) C. F. Izzard: Hydraulics of Runoff from Developed Surfaces, Proc. Highway Research Board, Vol. 26, 1946, pp. 129–150.
2) C. F. Izzard and M. T. Augustine: Preliminary Report on Analysis of Runoff Resulting from Simulated Rainfall on a Paved Plot, Trans. Amer. Geophy. Union, 1943, pp. 500–509.
3) W. W. Horner and S. W. Jens: Surface Runoff Determination from Rainfall without Using Coefficients, Trans. A. S. C. E., Vol. 107, 1942, pp. 1039–1117.
4) W. I. Hicks: A Method of Computing Urban Runoff, Trans. A. S. C. E., Vol. 109, 1944, pp. 1217–1268.
5) L. K. Sherman; Stream Flow from Rainfall by the Unit Graph Mcthod, ENR, Vol. 108, 1932, pp. 501–505.
6) Ray K. Linsley, Jr., Max A. Kohler and Joseph L. Paulhus: Applied Hydrology, McGraw-Hill Book Co., Inc., New York, N. Y., 1949, p. 275.
7) Y. Iwagaki: On the Fundamental Equations for the Mean Flow of Water in Open Channels, Jour. J. S. C. E., Vol. 39, No. 10, 1954, pp. 26–30 (in Japanese).
8) F. F. Escoffier: A Graphical Method for Investigating the Stability of Flow in Open Channels or in Closed Conduits Flowing Partly Full, Trans. Amer. Geophy. Union, Vol. 31, No. 4, 1950, pp. 583–586.
9) S. Uchida: On the Analysis of Flood Wave in Reservoir by the Method of Characteristics, Proc. 2nd Japan National Congress for Appl. Mech., 1952, pp. 271–276.
10) H. Rouse: Engineering Hydraulics, John Wiley & Sons, Inc., New York, N. Y., 1950, p. 699.
11) T. Ishihara, Y. Iwagaki and T. Goda: Studies on the Thin Sheet Flow (1st Report), Trans. J. S. C. E., No. 6, 1951, pp. 31–38 (in Japanese).
12) T. Sueishi: On the Flood Analysis by Characteristics, Trans, J. S. C. E., No. 30. 1955 (in Japanese, in printing).

Publications of the Disaster Prevention Research Institute

The Disaster Prevention Research Institute publishes reports of the research results in the form of bulletins. Publications not out of print may be obtained free of charge upon request to the Director, Disaster Prevention Research Institute, Kyoto University, Kyoto, Japan.

Bulletins :

No. 1 On The Propagation of Flood Waves by Shoitiro Hayami, 1951.
No. 2 On the Effect of Sand Storm in Controlling the Mouth of the Kiku River by Tojiro Ishihara and Yuichi Iwagaki, 1952.
No. 3 Observation of Tidal Strain of the Earth (Part I) by Kenzo Sassa, Izuo Ozawa and Soji Yoshikawa. And Observation of Tidal Strain of the Earth by the Extensometer (Part II) by Izuo Ozawa, 1952.
No. 4 Earthquake Damages and Elastic Properties of the Ground by Ryo Tanabashi and Hatsuo Ishizaki, 1953.
No. 5 Some Studies on Beach Erosions by Shoitiro Hayami, Tojiro Ishihara and Yuichi Iwagaki, 1953.
No. 6 Study on Some Phenomena Foretelling the Occurrence of Destructive Earthquakes by Eiichi Nishimura, 1953.
No. 7 Vibration Problems of Skyscraper. Destructive Element of Seismic Waves for Structures by Ryo Tanabashi, Takuzi Kobori and Kiyoshi Kaneta, 1954.
No. 8 Studies on the Failure and the Settlement of Foundations by Sakuro Murayama, 1954.
No. 9 Experimental Studies on Meteorological Tsunamis Traveling up the Rivers and Canals in Osaka City by Shoitiro Hayami, Katsumasa Yano, Shohei Adachi and Hideaki Kunishi, 1955.
No. 10 Fundamental Studies on the Runoff Analysis by Characteristics by Yuichi Iwagaki, 1955.

Bulletin No. 10 Published December, 1955

昭和 30 年 12 月 5 日 印刷
昭和 30 年 12 月 10 日 発行
編輯兼発行者 京都大学防災研究所
印刷者 山代多三郎
京都市上京區寺之内通小川西入
印刷所 山代印刷株式会社